Horseradish Peroxidase Transport Across Rat Alveolar Epithelial Cell Monolayers

Yasuhisa Matsukawa,[1,8] Hiroshi Yamahara,[1,8] Vincent H. L. Lee,[1,2] Edward D. Crandall,[3,4,5] and Kwang-Jin Kim[3,5,6,7,9]

Received March 19, 1996; accepted June 25, 1996

Purpose. To evaluate the transport characteristics of horseradish peroxidase (HRP, a nonspecific fluid-phase endocytosis marker) across an in vitro model of tight (>2,000 ohm-cm^2) rat alveolar epithelial cell monolayers grown on tissue culture-treated polycarbonate filters.

Methods. Unidirectional HRP fluxes were estimated from the appearance rate of HRP in the receiver fluid following instillation in the donor fluid as a function of donor [HRP] and temperature. Molecular species present in either bathing fluid were determined at the end of flux experiments using fluorescein isothiocyanate (FITC)-labeled HRP by gel permeation chromatography. Cell-associated HRP activity at the end of the transport experiment was determined, as were the rates of recycling and transcellular movement of HRP. An enzymatic assay was used to quantify HRP activity in the bathing fluid and cells.

Results. Unidirectional HRP fluxes were symmetric and increased linearly with up to 50 μM donor [HRP]. The apparent permeability coefficient of HRP was reduced by 3.5 times upon lowering the temperature from 37 to 4°C. About 50% of the FITC-labeled species present in either receiver fluid was intact HRP. Cell-associated HRP estimated from apical HRP incubation was about 4 times greater than that from basolateral incubation. Recycling into apical fluid of cell-associated HRP following apical incubation occurred rapidly with a half-time ($T_{1/2}$) of ~5 min, reaching a plateau at ~67% of the initial cell-associated HRP, while transcellular movement of HRP (into basolateral fluid) took place with a $T_{1/2}$ of ~20 min, attaining a steady-state at ~13% of the initial cell-associated HRP. Basolateral recycling of HRP was also rapid ($T_{1/2}$ = ~5 min) reaching a steady-state at ~35% of the initial basolaterally-bound HRP. Transcellular movement of HRP following basolateral incubation was slower ($T_{1/2}$ = ~70 min), leveling off at 50% of the initial cell-associated HRP.

Conclusions. HRP appears to be transported relatively intact (~50%) across rat alveolar epithelial barrier via nonspecific fluid-phase endocytosis. The transepithelial pinocytotic rate of alveolar epithelial cells is estimated to be about 25 nL/cm^2/h.

KEY WORDS: protein transport; pinocytosis; fluid-phase endocytosis; alveolar epithelium; drug delivery.

[1] Department of Pharmaceutical Sciences, University of Southern California, Los Angeles, California.
[2] Department of Ophthalmology, University of Southern California, Los Angeles, California.
[3] Department of Medicine, University of Southern California, Los Angeles, California.
[4] Department of Pathology, University of Southern California, Los Angeles, California.
[5] Will Rogers Institute Pulmonary Research Center, University of Southern California, Los Angeles, California.
[6] Departments of Physiology and Biophysics, University of Southern California, Los Angeles, California.
[7] Department of Biomedical Engineering, University of Southern California, Los Angeles, California.
[8] Present Address: Tanabe Seiyaku Co., Ltd., Pharmaceutics Research Laboratory, 16-89, Kashima 3 chome, Yodogawa-ku, Osaka 532, Japan.
[9] To whom correspondence should be addressed.

INTRODUCTION

Alveolar epithelium lines the distal airspaces of the lung and provides high resistance to the leakage of solutes and fluid from the surrounding interstitial and vascular spaces, as suggested by a number of physiological and morphological studies (1,2). This property of high resistance helps keep the alveolar airspaces of the lung relatively fluid-free for efficient gas exchange. Moreover, active Na^+ absorption from the apical fluid across the alveolar epithelial barrier has been reported to play a major role in the maintenance of alveolar fluid balance (3).

Proteins are important constituents of epithelial lining fluid of distal airspaces of the lung. Immunohistochemical and biochemical studies have revealed the presence of serum proteins (e.g., albumin and immunoglobulins) in bronchoalveolar lavage fluid and on the surface of the respiratory epithelium lining the distal airspaces (4). The mechanisms and pathways for protein translocation across the alveolar epithelium *per se* have not been well characterized to date.

In this study, the transepithelial transport properties of horseradish peroxidase (~40,000 daltons, a fluid-phase endocytosis (i.e., nonspecific pinocytosis) marker) have been investigated to shed some light on the pinocytotic capacity of the alveolar epithelial barrier in relation to transport of therapeutic proteins of the size comparable to HRP. We measured the rate of transepithelial transport and cellular metabolism of HRP in the alveolar epithelial barrier utilizing an in vitro model of rat alveolar epithelial cell monolayers in primary culture. These monolayers have been reported to exhibit phenotypic and morphological characteristics expected for in vivo alveolar epithelium (5,6).

MATERIALS AND METHODS

Materials

Horseradish peroxidase (HRP) and fluorescein isothiocyanate (FITC)-labeled HRP were purchased from Sigma Chemical Co. (St. Louis, MO). Cell culture media and supplies were obtained from Gibco (Grand Island, NY). All other chemicals were of the highest purity available commercially.

Primary Culture of Rat Alveolar Epithelial Cell Monolayers

We have previously reported our approach to the routine generation of "tight" monolayers of rat pneumocytes in primary culture (3,7). Briefly, lungs of male, specific pathogen-free, Sprague-Dawley rats (~150 g) were perfused, lavaged, and treated with 2.5 U/mL of porcine pancreatic elastase (Worthington, Freehold, NJ) for 20 min at 37°C. Lungs were then minced to yield tissue blocks (about 1 mm^3) which were filtered sequentially through 150 and 35 μm Nitex (Tetko, Elmsford, NY) membranes. The filtered crude cell mixture was further purified

0724-8741/96/0900-1331$09.50/0

by immunoglobulin G (IgG) panning methods (3,7) which yield >90% type II pneumocytes. These purified type II pneumocytes were resuspended in a culture medium (Earle's modification of minimum essential medium supplemented with 10% newborn bovine serum, 100 U/mL penicillin, and 100 ng/mL streptomycin) and plated onto tissue culture-treated polycarbonate filter-inserts (1.13 cm^2, Transwell, Costar, Pleasanton, CA) at 1.2 × 10^6 cells/cm^2 (on day 0). Beginning about day 3 in culture, these alveolar epithelial cells-on-filters were confluent and exhibited morphological features akin to those of in vivo type I pneumocytes (e.g., protruding nuclei with thin cytoplasmic extensions of less than 0.5 μm thickness) and reactivity to a rat type I cell-specific monoclonal antibody (6).

Measurement of Bioelectric Properties

The primary cultured monolayers of rat alveolar pneumocytes were used on day 4. Monolayers contained in 12-well clusters were washed twice with pre-equilibrated (37°C, pH 7.4) Ringer's solution on both sides and allowed to stabilize with the new bathing medium for 2 h in a humidified incubator (5% CO_2 in air, 37°C). The Ringer's solution contained 116.40 mM NaCl, 5.40 mM KCl, 0.78 mM NaH_2PO_4, 25.00 mM $NaHCO_3$, 1.80 mM $CaCl_2$, 0.81 mM $MgSO_4$, 5.55 mM glucose, 15.00 mM N-[2-hydroxyethyl]-piperazine-N'-[2-ethanesulfonic acid] (HEPES), and 75 μM bovine serum albumin. The spontaneously generated transepithelial electrical potential difference (PD) and monolayer resistance (R) were monitored with a MilliCell ERS device (Millipore, Marlborough, MA). We used PD as an index of net active ion transport and R as an index of the integrity of tight junctions of the alveolar epithelial cell monolayer. These measurements were performed in both the absence and presence of up to 50 μM HRP in either apical or basolateral bathing fluid.

Measurement of Unidirectional HRP Fluxes and Cell-Associated HRP

Following 2 h equilibration with Ringer's solution, measurements of unidirectional HRP fluxes across the monolayers were initiated by spiking either apical (0.6 mL) or basolateral (1.5 mL) donor fluid with a dosing solution to yield up to a final (unlabeled) HRP concentration of 50 μM. Samples (1/10th of the corresponding reservoir volume) from the receiver fluid were taken at 0, 0.5, 1, 2, 3, and 4 h after the instillation of HRP to the donor fluid. An equal volume of fresh Ringer's solution was replenished after each sampling to keep the reservoir volumes constant. Control experiments show that there are no appreciable changes in bioelectric properties following these experimental maneuvers. Transepithelial HRP fluxes (J) were estimated from known concentration of HRP in the donor fluid and the amount of cumulative HRP appearing in the receiver fluid as a function of time. Apparent permeability coefficients (Papp) for HRP were estimated from the relationship, Papp = J/dC, where dC is the concentration gradient across the monolayer.

To estimate cell-associated HRP activity at the end of flux measurements, exposed cell monolayers were washed three times with ice-cold phosphate-buffered saline (pH 7.2). Cell-associated HRP was extracted by 30 min incubation of washed cell monolayers with an ice-cold lysis buffer containing 1% (v/v) Triton x-100, 0.5% (w/v) sodium dodecyl sulfate (SDS), 2 mM freshly made phenylmethylsulfonylfluoride (PMSF), 2 mM benzamidine, and 400 U/ml aprotinin. One hundred microliters of the cell lysate were used for HRP activity assay as described above. A standard curve for the HRP activity in cell lysate was generated using known concentrations of HRP under otherwise identical conditions.

HRP activity in the bathing fluids and cells was quantitated by an enzymatic assay reported by Herzog and Fahimi (8). Briefly, 100 μL of sample solution and 1 mL of 0.01 M phosphate buffer (pH 7.2) containing 0.01% 3,3'-dimethoxybenzidine and 0.01% (v/v) hydrogen peroxide are mixed in a cuvet (3 mL, thermostated at 37°C). The absorbance of the sample mixture was monitored continuously for 3 min at 460 nm in a spectrophotometer (Shimadzu UV-2101PC, Kyoto, Japan) and the activity of HRP estimated from the tangential line (i.e., slope) at time t = 0 of the absorbance measurements. Standard curves are similarly generated using known concentrations of HRP.

Measurements of Kinetic Parameters of HRP Transport

To determine the rates of internalization, recycling (i.e., effluxes), and transcellular movement of HRP, cultured pneumocyte monolayers were pre-incubated on ice/water (~4°C) for 4 h (with bathing fluid pH kept near 7.4) at 50 μM HRP in either apical or basolateral donor fluid and subsequently washed with ice-cold, HRP-free Ringer's solution three times (5 min incubation each). These monolayers were then bathed on both sides with pre-warmed (37°C) HRP-free Ringer's solution. The accumulation of HRP in the ipsilateral and contralateral reservoir fluids was monitored at 0, 5, 15, 30, 60, 120, 180, and 240 min following placement of the washed cell monolayers into a 37°C incubator. The activity of HRP remaining with the cells at these time points was also measured by the enzymatic assay described earlier. Relative HRP efflux rates were calculated according to the relationship, efflux rate (%) = 100 * (amount of HRP in either the apical or basolateral bathing fluid)/(total HRP), where total HRP at a given time point was the sum of the cell-associated HRP and that appearing in both apical and basolateral fluids.

Determination of the Fraction of Intact FITC-HRP in Bathing Fluids

In order to quantify the cellular processing of HRP, the donor and receiver bathing fluid samples were collected following 4 h FITC-HRP flux measurements at 25 μM donor concentration and subjected to gel permeation chromatography (GPC) with fluorescence detection. Prior to chromatography, bathing fluid samples were concentrated in a rotary evaporator, resuspended with 200 μL of MilliQ water (Millipore, Marlborough, MA), and injected (150 μL) into a high performance liquid chromatography (HPLC) system. The dosing solution was similarly treated. The HPLC system consisted of a dual pump, controller, and a variable wavelength UV detector (all from Waters, Milford, MA), and a fraction collector (LKB-Pharmacia, Farmington, NJ). A GPC column used was 300WS Protein Pack (Waters, Milford, Boston, MA) and the flow rate was 1 mL/min. The mobile phase was phosphate-buffered saline (pH 7.2) diluted 10 times with MilliQ water. One milliliter

fractions of the eluant were measured for fluorescence (Perkin Elmer 650-10S, Norwalk, CT) at excitation and emission wavelengths of 490 nm and 520 nm, respectively.

Statistical Analyses

Data are presented as mean ± S.E.M. (n), where n is the number of observations.

Differences among group means are determined by one-way analyses of variance with modified post-hoc Newman-Keuls procedures (9). Where appropriate, unpaired Student's *t*-tests are used for comparing two group means. $p < 0.05$ is taken as the level of significance.

RESULTS

The monolayers used in this study were obtained from 24 different preparations of alveolar epithelial cells. The monolayers showed 8.90 (±0.21) mV (apical-side as reference) of PD and 2.61 (± 0.054) kohm-cm^2 of R (n = 354), which were comparable to those reported by Kim et al. (3,7) previously. The presence of up to 50 μM HRP in either donor fluid elicited no significant effects on PD and R, indicating that the observed HRP fluxes were not due to the alterations in barrier properties of the alveolar epithelial cell monolayers. Preincubation of cell monolayers with 50 μM HRP at 4°C, followed by washing and rewarming, led to no appreciable changes in PD and R of the monolayers treated identically without HRP in the bathing fluids.

The time courses of HRP translocation at a 10 μM donor concentration across rat alveolar epithelial cell monolayers are shown in Figure 1, where the cumulative appearance of HRP in either receiver fluid increased linearly. No measurable lag time was observed in these time courses. As can be seen in Table 1, the HRP Papp ($\times 10^{-9}$ cm/sec) was neither direction- nor concentration-dependent for up to 50 μM donor HRP concentration investigated in this study. The Papp for HRP at 50 μM at 37°C decreased by about 70% from 7.21 (±1.16) (n = 3) and 7.34 (±1.56) (n = 3) to 2.03 (±0.38) (n = 3) and 2.14 (±0.10) (n = 3) for the AB and BA directions, respectively, upon lowering the temperature to 4°C. The Papp for HRP at 4°C was also not direction-dependent.

Table 1. HRP Transport Across Alveolar Epithelial Cell Monolayers (37°C, 4 h)[a]

Direction	Donor Concentration (μM)	Flux ($\times 10^{-5}$ pmol/cm^2/sec)	Papp ($\times 10^{-9}$ cm/sec)
AB[b]	10	6.69 ± 1.21	6.69 ± 1.21
	25	16.7 ± 2.20	6.67 ± 0.88
	50	36.1 ± 5.80	7.21 ± 1.16
BA[c]	10	6.88 ± 0.28	6.88 ± 0.28
	25	19.0 ± 2.98	7.60 ± 1.19
	50	36.7 ± 7.80	7.34 ± 1.56

[a] Entries are mean ± S.E. (n=3).
[b] Parameters measured in the apical-to-basolateral direction.
[c] Parameters measured in the basolateral-to-apical direction.

Figure 2 shows the chromatograms for basolateral receiver fluid which were pooled at the end of 4 h FITC-HRP flux measurements. About 45% of the fluorescence (based on the peak area under the curve) was attributable to FITC-HRP, whereas the remainder was associated with subfragments of HRP. Apical receiver fluid exhibited a similar chromatographic profile. Both apical and basolateral donor fluids revealed only a single major peak for intact FITC-HRP, as did the dosing solution (data not shown).

Cell-associated HRP linearly increased with donor [HRP] (Figure 3), where apical HRP incubation at each concentration led to cell-associated HRP about four times greater than that resulting from basolateral incubation. Figures 4 and 5 depict the time courses of HRP, where HRP was allowed to bind to the cell surface at 4°C, followed by subsequent measurements of the HRP remaining with cells and that appearing in the bathing fluids after warming the pre-exposed monolayer to

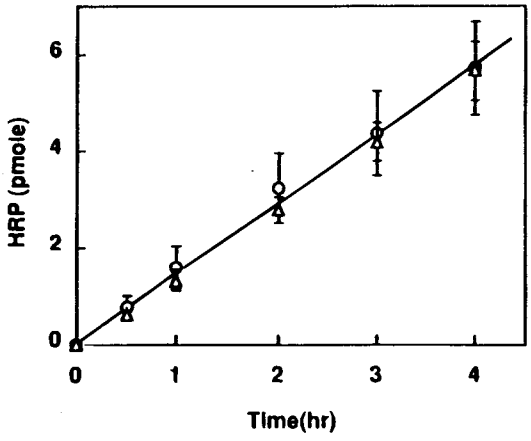

Fig. 1. Time courses of HRP accumulation in the receiver fluids at 10 μM HRP in the apical (o) or basolateral (△) donor fluids of rat alveolar epithelial cell monolayers. Each data point with a given symbol represents the mean, and the vertical bar on the symbol is the standard error of the mean.

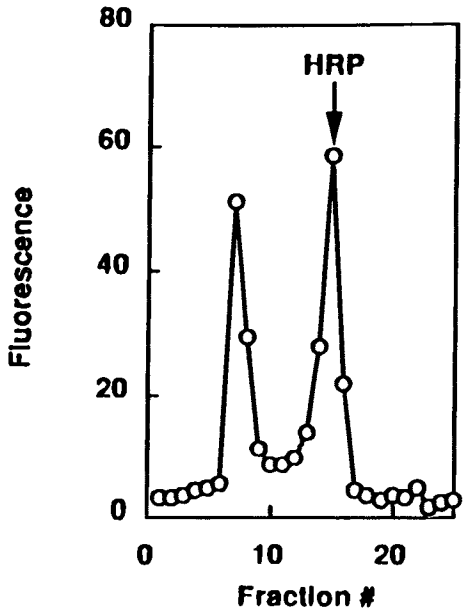

Fig. 2. Chromatogram for FITC in basolateral receiver fluid collected at the end of 4 h flux experiments with 25 μM donor FITC-HRP.

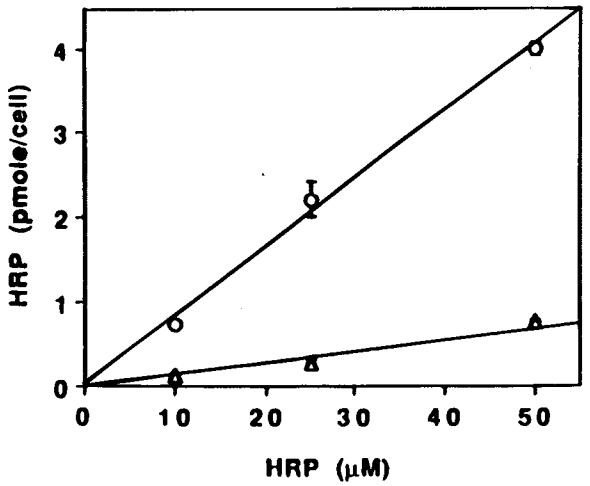

Fig. 3. Cell-associated of HRP estimated at the end of 4 h flux experiments as a function of HRP concentration in the apical (o) or basolateral (△) donor fluid of rat alveolar epithelial cell monolayers.

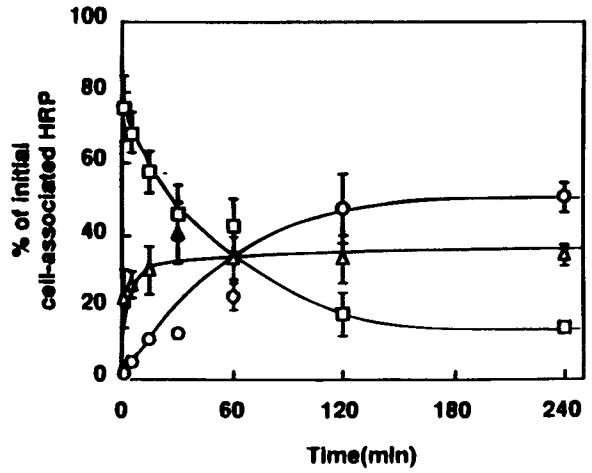

Fig. 5. Time courses of relative efflux rates and HRP activity remaining with the cell monolayer, following pre-exposure of cell monolayers to 50 μM HRP in the basolateral fluid. △: HRP released into (i.e., recycled to) basolateral fluid, ○: HRP transcytosed to apical fluid, □: HRP remaining with the cells.

37°C. The time courses of the relative rates of HRP appearing in the ipsilateral and contralateral bathing fluids and HRP remaining with the cell monolayer, following pre-exposure of the apical aspect of the monolayer to HRP, are shown in Figure 4. The rate of HRP appearing in the ipsilateral (i.e., apical) fluid rose to 67% of the initial (i.e., total) cell-associated HRP activity with a half time ($T_{1/2}$) of ~5 min, whereas the HRP remaining with the cell monolayer decreased to 20% of the initial value with a $T_{1/2}$ of ~18 min. HRP appearing in the contralateral fluid (i.e., the HRP translocated across cell monolayer in the AB direction) reached a plateau at 13% of the initial cell-associated HRP with a $T_{1/2}$ of ~20 min.

When the basolateral aspect of alveolar epithelial cell monolayers was pre-exposed to HRP (Figure 5), the release of HRP into the ipsilateral (i.e., basolateral) fluid was also rapid, with a $T_{1/2}$ of ~5 min and reaching a plateau at 35% of initial cell-associated HRP, whereas cell-associated HRP decreased to a steady-state at 15% of the initial value with a $T_{1/2}$ of ~37 min. The translocation of HRP across the cell monolayer to the contralateral fluid (i.e., in the BA direction) occurred with a $T_{1/2}$ of ~70 min, leveling off at 50% of the initial cell-associated HRP.

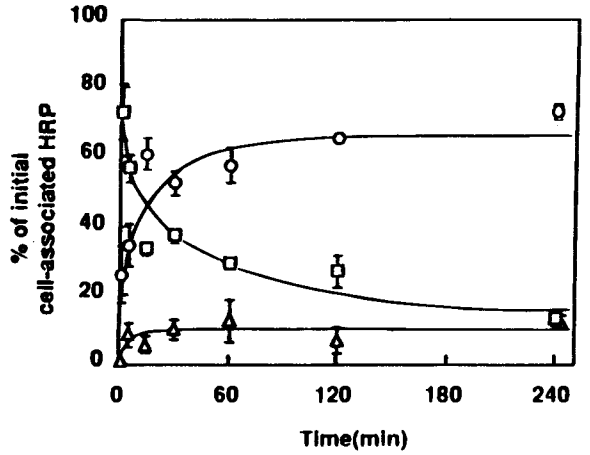

Fig. 4. Time courses of relative efflux rates and HRP activity remaining with the cell monolayer, following pre-exposure of cell monolayers to 50 μM HRP in the apical fluid. ○: HRP released into (i.e., recycled to) apical fluid, △: HRP transcytosed to basolateral fluid, □: HRP remaining with the cells.

DISCUSSION

In this study, we have shown that the rates of transepithelial HRP transport across rat alveolar epithelial cell monolayers are symmetric (Table 1 and Figure 1) and not dependent on HRP concentrations up to 50 μM (Table 1). The permeability coefficient of HRP in both the AB and BA directions across the alveolar epithelial barrier is $\sim 7.0 \times 10^{-9}$ cm/sec at 37°C, which was decreased by ~70% at 4°C. The strong dependency of HRP Papp on temperature suggests that HRP translocation is not likely to be limited by simple restricted diffusion via paracellular routes. If paracellular diffusion of HRP across the cell monolayer was the predominant transport mechanism, HRP Papp at 4°C is expected to decrease by about 40% from that at 37°C. Our data are therefore consistent with translocation of intact (i.e., enzymatically-active) HRP across the alveolar epithelial barrier, taking place most likely via non-saturable vesicular pathways (e.g., pinocytosis).

The HRP Papp estimated in this study is about two orders of magnitude smaller than the Papp of $\sim 1.8 \times 10^{-7}$ cm/sec for mannitol (a paracellular transport marker) (3) and about one order of magnitude smaller than the Papp of $\sim 2.5 \times 10^{-8}$ cm/sec for inulin (a polysaccharide of about 5 kDa) (10). On the other hand, Papp of 3.7×10^{-10} cm/sec for HRP was reported for filter-grown Madin-Darby canine kidney (MDCK) cell monolayers (with resistance >3 kohm-cm^2) (11).

The pinocytosis rate estimated from the observed translocation of intact HRP across the alveolar epithelial barrier is ~25n L/cm^2/h (or ~0.25 pmole/cm^2/h at 10 μM), which is about 1–2 orders of magnitude smaller than that reported for rabbit and mouse intestinal epithelial cells utilizing the same transport marker (12,13). For example, MDCK cells have been reported

to have ~200 nL/cm^2/h of pinocytosis (14). In the human colon carcinoma cell line Caco-2, HRP undergoes bidirectional transcytosis via non-specific (i.e., fluid-phase) endocytosis at a rate of ~27 pmole/cm^2/h at 10 μM donor concentration (15). Assuming a surface area of ~100 m^2 for human alveolar airspaces, ~0.025 L/h of fluid may be translocated by pinocytosis across the alveolar epithelial barrier of the lung. By contrast, active Na^+ removal across the alveolar epithelial barrier of the adult human lung may result in resorption of ~0.17 L/h of isotonic fluid (3). Thus, the contribution of the pinocytotic route at baseline to overall transalveolar epithelial movement of water appears to be small (about 15%) compared to that occurring secondary to active sodium resorption.

Cell-associated HRP estimated at 4°C following apical incubation is about four times greater than that following basolateral incubation (Figure 2). The larger apical binding of HRP may be due to the interaction of HRP with cell surface components (e.g., glycocalyx) present in alveolar epithelial cells. The interaction of HRP with these components, however, appears to be rather weak, since a substantial proportion (~35 to 65%) of the cell-associated HRP is rapidly (with a $T_{1/2}$ of about 5 min) released back to the ipsilateral fluid (Figures 4 and 5).

The $T_{1/2}$ of about 20 min for transcellular HRP movement in the AB direction is about four times faster than that occurring in the opposite direction (Figures 4 and 5), whereas the overall transcytotic rates of HRP in both directions are the same (Table 1 and Figure 1). However, the fraction of initial cell-associated HRP which was translocated across the monolayer at steady-state is greater in the BA direction (50%) than that in the AB direction (13%) (Figures 4 and 5). This apparent disparity can be explained by the observed kinetic parameters and the four-fold difference in cell-associated HRP activities for apical and basolateral HRP incubations (Figure 2). If 100 molecules of cell-associated HRP is assumed for apically-exposed monolayers, about 13 molecules are translocated in the AB direction at steady-state. By contrast, the cell-associated HRP observed from the basolateral HRP incubation is about 25% of that observed for apical incubation at the same HRP donor concentration (Figure 2) (i.e., 25 molecules), about half of which will be translocated at steady-state across the cell monolayer in the BA direction, or $25 \times 0.5 = 12.5$ molecules. Thus, the overall translocation of HRP observed at steady-state in both directions is approximately the same, which is consistent with the same rates of transepithelial pinocytosis for intact HRP observed in either direction.

About half of the FITC-labeled substances present in either the apical or basolateral receiver fluid at 4 h flux measurements are associated with intact HRP (Figure 3), suggesting that part of the internalized HRP undergoes cellular metabolism (most likely in the lysosomal compartment). The fraction of internalized HRP undergoing cellular metabolism is ~50% in alveolar epithelial cells, as opposed to >90% in mouse jejunal cells (12). Similar profile of lysosomal degradation of HRP was found in rabbit jejunum, where only 3% of the total absorptive flux of ^{3}H-labeled substances was associated with intact HRP (13). These data indicate that alveolar epithelial metabolism of exogenous proteins which are internalized via pinocytotic route is relatively small (~50%) compared to that (90 to 97%) occurring in intestinal epithelial cells.

In summary, the alveolar epithelial barrier at baseline appears to have a limited pinocytotic rate. Although the kinetic profiles of alveolar epithelial HRP transport in both AB and BA directions are dissimilar, the overall rates of transepithelial pinocytosis at steady-state in either direction are the same. It is likely that exogenous proteins (of size comparable to or greater than HRP and lacking specialized transport processes (e.g., receptor-mediated transcytosis)) are translocated with a similar rate via fluid-phase endocytosis across the alveolar epithelial barrier. The role of such nonspecific fluid-phase endocytosis in overall peptide/protein drug absorption into the systemic circulation remains to be determined, as does the regulation of alveolar epithelial pinocytosis.

ACKNOWLEDGMENTS

The authors acknowledge the skillful assistance of Martha Jean Foster, Monica Flores, Stephanie M. Zabski, and Stacey Scherer. Dr. Vincent H.L. Lee is Herbert Gavin Professor of Pharmaceutical Sciences. Dr. Edward D. Crandall is Hastings Professor of Medicine. This study was supported in part by Hastings Foundation and National Institutes of Health Research Grants HL38578, HL38621, HL38658, GM52812, and CA37528.

REFERENCES

1. M. M. Berg, K. J. Kim, R. L. Lubman, and E. D. Crandall. Hydrophilic solute transport across rat alveolar epithelium. *J. Appl. Physiol.* **66**:2320–2327 (1989).
2. E. E. Schneeberger, and M. J. Karnovsky. The ultrastructural basis of alveolar-capillary membrane permeability to peroxidase used as a tracer. *J. Cell Biol.* **37**:781–793 (1968).
3. K. J. Kim, J. M. Cheek, and E. D. Crandall. Contribution of Na^+ and Cl^- fluxes to net ion transport by alveolar epithelium. *Respir. Physiol.* **85**:245–256 (1991).
4. J. Bignon, M. C. Jaurand, M. C. Pinchon, C. Spain, and J. M. Waynet. Immunoelectron microscopic and immunochemical demonstrations of serum proteins in the alveolar lining material of the rat lung. *Am. Rev. Respir. Dis.* **113**:109–120 (1976).
5. J. M. Cheek, M. J. Evans, and E. D. Crandall. Type I cell-like morphology in tight alveolar epithelial monolayers. *Exp. Cell Res.* **84**:375–387 (1989).
6. S. I. Danto, S. M. Zabski, and E. D. Crandall. Reactivity of alveolar epithelial cells in primary culture with type I cell monoclonal antibodies. *Am. J. Respir. Cell Mol. Biol.* **6**:296–306 (1992).
7. K. J. Kim, D. J. Suh, R. L. Lubman, S. I. Danto, Z. Borok, and E. D. Crandall. Ion fluxes across alveolar epithelial cell monolayers. *J. Tissue. Cult. Meth.* **14**:187–184 (1992).
8. V. Herzog, and H. D. Fahimi. A new sensitive colorimetric assay for peroxidase using 3,3′-diaminobenzidine as hydrogen donor. *Anal. Chem.* **55**:554–562 (1973).
9. B. J. Winer. *Statistical Principles in Experimental Design*, McGraw-Hill, New York, 1971.
10. K. J. Kim, and E. D. Crandall. Heteropore populations of bullfrog alveolar epithelium. *J. Appl. Physiol.* **54**:140–146 (1983).
11. C. H. von Bonsdorff, S. D. Fuller, and K. Simons. Apical and basolateral endocytosis in Madin-Darby canine kidney (MDCK) cells grown on nitrocellulose filters. *EMBO J.* **4**:2781–2792 (1985).
12. M. Heyman, R. Ducroc, J.-F. Desjeux, and J. L. Morgat. Horseradish peroxidase transport across adult rabbit jejunum in vitro. *Am. J. Physiol.* **242**:G558–G564 (1982).
13. M. Heyman, A. M. Crain-Denoyelle, and J. F. Desjeux. Endocytosis and processing of protein by isolated villus and crypt cells of the mouse small intestine. *J. Pediatr. Gastroenterol. Nutr.* **9**:238–245 (1989).
14. M. J. Cho, D. P. Thompson, C. T. Cramer, T. J. Vidmar, and J. F. Scieszka. The Madin Darby canine kidney (MDCK) epithelial cell monolayer as a model cellular transport barrier. *Pharm. Res.* **6**:71–77 (1989).
15. M. Heyman, A.-M. Crain-Denoyelle, S. K. Nath, and J.-F. Desjeux. Quantification of protein transcytosis in the human colon carcinoma cell line Caco-2. *J. Cell. Physiol.* **143**:391–395 (1990).